

Variation of magnetoresistance in $\text{Ni}_{2+x}\text{Mn}_{1-x}\text{Ga}$ with composition

S. Banik,¹ Sanjay Singh,¹ R. Rawat,¹ P. K. Mukhopadhyay,² B. L. Ahuja,³ A. M. Awasthi,¹ S. R. Barman,^{1,a)} and E. V. Sampathkumaran⁴

¹UGC-DAE Consortium for Scientific Research, Khandwa Road, Indore 452001, India

²LCMP, S. N. Bose National Centre for Basic Sciences, Kolkata 700098, India

³Department of Physics, M. L. Sukhadia University, Udaipur 313001, India

⁴Tata Institute of Fundamental Research, Mumbai 400005, India

The magnetoresistance (MR) of $\text{Ni}_{2+x}\text{Mn}_{1-x}\text{Ga}$ ($-1 \leq x \leq 0.35$) ferromagnetic shape memory alloy shows a large increase in magnitude at room temperature (RT) with increasing x . For Mn_2NiGa ($x=-1$), MR at 8 T is -0.2% , while for $\text{Ni}_{2.35}\text{Mn}_{0.65}\text{Ga}$ ($x=0.35$), it is -7.3% . Thus, MR of $\text{Ni}_{2+x}\text{Mn}_{1-x}\text{Ga}$ can be varied over one order of magnitude by changing composition (x). Considering that the Curie temperature (T_C) varies with x , the MR behavior in the austenitic phase is explained on the basis of the $s-d$ scattering model. By fitting the MR at 8 T in the austenitic phase for different x and T , a $(T/T_C)^6$ power law dependence is obtained. In contrast to the monotonic MR variation with x , the magnetization at RT is highest for Ni_2MnGa ($x=0$) and decreases for both Ni and Mn excess compositions.

I. INTRODUCTION

The large magnetic field induced strain exhibited by $\text{Ni}_{2+x}\text{Mn}_{1-x}\text{Ga}$ ferromagnetic shape memory alloys has started a flurry of activity in this area.¹ Besides the actuation behavior, findings that Ni–Mn–Ga exhibits giant magnetocaloric effect² and negative magnetoresistance (MR)^{3,4} renders it as an important material for technological applications. Biswas *et al.*³ studied the MR of the bulk ingot of Ni_2MnGa at different temperatures corresponding to the austenitic, pre-martensitic and martensitic phases and for $\text{Ni}_{2.1}\text{Mn}_{0.9}\text{Ga}$, 5% negative MR was reported at 300 K and 8 T.³ A characteristic cusplike shape of MR(H) observed in the low field in the martensitic phase well below the Curie temperature (T_C , $T/T_C=0.4$) was ascribed to the presence of twin and domain structures. Recently, a negative to positive to negative switching behavior of MR with decreasing temperature has been reported for a Mn excess $\text{Ni}_{2+x}\text{Mn}_{1-x}\text{Ga}$ composition: $\text{Ni}_{1.75}\text{Mn}_{1.25}\text{Ga}$.⁴ This is one of the unique compositions in the $\text{Ni}_{2+x}\text{Mn}_{1-x}\text{Ga}$ family that has low martensitic transition temperature of about 76 K. This enables the study of the ferroelastic transition much below the Curie temperature ($T_C=380$ K), where $s-d$ scattering is negligible. In the austenitic phase, the negative MR was related to $s-d$ scattering. However, below 135 K ($T/T_C=0.35$), where $s-d$ scattering is negligible, MR was found to be positive (0.3%); while below the martensitic transition ($T/T_C=0.2$), the negative MR was ascribed to a decrease in electron scattering at the twin boundaries and domain walls with the application of magnetic field.⁴

The properties of $\text{Ni}_{2+x}\text{Mn}_{1-x}\text{Ga}$ are dependent on composition, and the transition temperatures in particular, vary to a large extent on x .⁵⁻⁷ Doping Ni in place of Mn in $\text{Ni}_{2+x}\text{Mn}_{1-x}\text{Ga}$ decreases the Curie temperature (T_C) from 376 to 325 K, but increases the martensitic start temperature

(T_M) from 210 to 325 K between $x=0$ and 0.2. At $x=0.2$, T_C and T_M merge, while for $x>0.2$, T_M is larger than T_C .⁶ In Mn excess compositions, T_M exhibits a nonmonotonic variation, whereas T_C increases monotonically with Mn content.⁷ These changes in properties prompted us to study MR in a series of well characterized $\text{Ni}_{2+x}\text{Mn}_{1-x}\text{Ga}$ bulk alloys spanning both the Ni excess and Mn excess regions of the phase diagram for $-1 \leq x \leq 0.35$. We find that the MR at room temperature (RT) decreases by more than an order of magnitude from Ni excess ($x=0.35$) to Mn excess ($x=-1$) compositions. Such large change in MR could have important practical application as magnetic sensors. In fact, a composition spread of Ni–Mn–Ga thin film has been grown on Si wafer and studied using scanning superconducting quantum interference device (SQUID) and microdiffraction.⁸ We explain the variation of MR in the austenitic phase for different x at $T \leq 300$ K by the theoretical calculation of Kataoka⁹ based on $s-d$ scattering model. Close to T_C ($T/T_C \approx 0.9$), although in the martensitic phase, MR is dominated by $s-d$ scattering, while considerably below T_C it is shown to deviate.

II. EXPERIMENTAL DETAILS

The polycrystalline ingots of $\text{Ni}_{2-x}\text{Mn}_{1+x}\text{Ga}$ ($-1 \leq x \leq 0.35$) have been prepared by melting appropriate quantities of Ni, Mn, and Ga (99.99% purity) in an arc furnace. The ingots are then annealed at 1100 K for 9 days for homogenization and subsequently quenched in ice water.⁶ The specimens with $x>0.35$ have not been studied since they have more than one structural phases.¹⁰ The energy dispersive analysis of x rays has been used to determine the composition. The ingots have been further characterized by x-ray diffraction (XRD), differential scanning calorimetry (DSC), magnetization, and ac susceptibility measurements.^{6,10,11} All the peaks in the XRD pattern could be indexed as cubic $L2_1$ structure for the austenitic phase and as tetragonal or modulated structure for the martensitic phase. Resistivity and MR have been performed as functions of field at different tem-

^{a)}Electronic mail: barmansr@gmail.com.

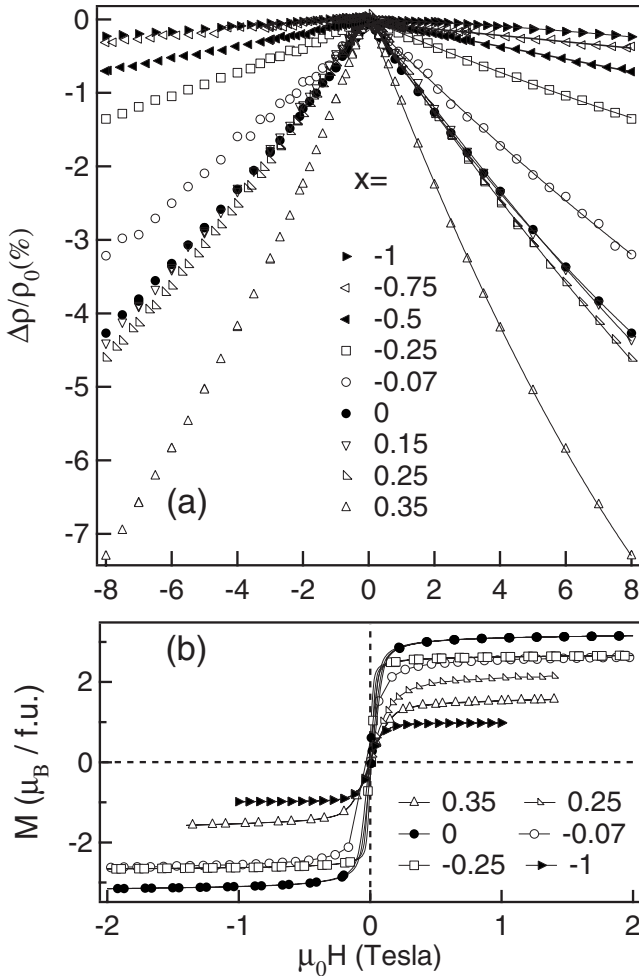


FIG. 1. Isothermal (a) MR and (b) M - H loops as a function of field for $\text{Ni}_{2+x}\text{Mn}_{1-x}\text{Ga}$ ($-1 \leq x \leq 0.35$) at RT (300 K). Solid lines in (a) are fit to the data (see text).

peratures. A maximum $\mu_0 H$ of 8 T was used for carrying out the longitudinal MR measurements using a magnet from Oxford Instruments Inc., U.K. For MR measurement, $\mu_0 H$ is varied from 0 to 8 to -8 to 0 T. MR is calculated using the formula $\Delta\rho_m = \Delta\rho/\rho_0 = (\rho_H - \rho_0)/\rho_0$, where ρ_H and ρ_0 are the resistivity in field H and zero, respectively. The magnetization measurements have been performed in a SQUID (MPMS XL5) magnetometer. The martensitic start temperature (T_M) has been determined by DSC, while T_C has been determined by magnetization and ac susceptibility measurements. T_C for Mn excess specimens and magnetization for $x = -0.5$ and -0.75 have been taken from literature.⁷

III. RESULTS AND DISCUSSION

Isothermal MR data for $\text{Ni}_{2+x}\text{Mn}_{1-x}\text{Ga}$ as a function of field at RT are shown in Fig. 1(a). The data for $x = 0$ and 0.15 are in agreement with our previously published work.³ In Ref. 3, we concentrated on the change in MR(H) shape in different phases as a function of temperature, while here we study the whole range of compositions with varying Ni to Mn ratio mostly in the austenitic phase. MR is negative at RT for all specimens, but exhibits a monotonic increase in magnitude from 0.2% to 7.3% at 8 T, as x increases from

-1 (Mn_2NiGa) to 0.35 ($\text{Ni}_{2.35}\text{Mn}_{0.66}\text{Ga}_{0.98}$). Thus, more than 35 times increase in MR is obtained. The variation of MR with magnetic field has been fitted by a second order polynomial of the form $\alpha(\mu_0 H) + \beta(\mu_0 H)^2$ [solid lines in Fig. 1(a)]. β/α varies between 0.03 and 0.09, where for a straight line $\beta/\alpha = 0$ and for a perfect parabola it should be infinity. Thus, small values of β/α indicate that the dependence of MR on H is nearly linear. As a consequence of this, even at moderate fields such as 2 T, MR increases with x , although the extent of variation is smaller than at 8 T.

At RT, all the studied compositions ($-1 \leq x \leq 0.35$) are in the magnetic state, as depicted by the isothermal hysteresis loops that are very narrow with the coercive field of 4–8 mT [Fig. 1(b)]. Comparison of Figs. 1(a) and 1(b) shows that the variation of MR with magnetic field does not track isothermal magnetization. The linearity of MR(H) has been reported in Ni–Mn–Ga and other Mn based ferromagnetic systems.^{3,4,12,13} For Ni–Mn–Ga, nearly linear MR(H) up to 8 T at temperatures not far below T_C has been ascribed to s - d scattering^{3,4} based on the theoretical calculation of MR for ferromagnetic metals.⁹ However, linear nonsaturating behavior of MR for ferromagnets (Ni, Fe, and Co) above saturation of magnetization up to 40 T has been observed and ascribed to electron-magnon scattering and the spin-wave damping in high fields.¹⁴ Such high field MR studies on Ni–Mn–Ga will be interesting to perform in future and is outside the scope of the present work.

Negative MR for magnetic metals has been explained on the basis of s - d scattering model where s conduction electrons are scattered by localized d spins on the magnetic ions.^{9,15} In presence of two overlapping s and d bands at the Fermi energy, the scattering may occur within a single band or may involve s - d transitions. The decrease in the resistivity below T_C is ascribed to the decrease in s - d scattering by the development of the magnetic order. In the magnetic state, in absence of an external magnetic field, the s - d scattering increases as T approaches T_C because the magnetic fluctuations increase. However, application of magnetic field suppresses the fluctuations and as a result the s - d scattering decreases resulting in decrease in ρ . Thus, due to s - d scattering, $\rho(H)$ decreases substantially resulting in large MR at T less than but close to T_C , whereas for $T \ll T_C$ the magnetic fluctuations are small and hence MR would be small.

Kataoka⁹ performed detailed theoretical calculation based on the s - d scattering model using Boltzmann theory for ferromagnetic metals. In particular, the difference between the two types of carriers consisting of up and down-spin electrons was explicitly taken into account and their relaxation times were determined self-consistently. Ni_2MnGa is a full Heusler alloy and such alloys are known to be ideal local moment ferromagnets with the moments localized on Mn atoms. The localized character of Mn moments arises from the exclusion of minority spin electrons from the Mn 3d shell.¹⁶ Our recent spin polarized density of states calculations for Ni_2MnGa (Ref. 17) and Mn_2NiGa (Ref. 18) also confirms this. In Ref. 9, ρ in zero ($H/H_C = 0$) and finite external magnetic field ($H/H_C > 0$, H_C is a measure of the magnetic field given by $k_B T_C / g \mu_B$) have been calculated as a function of T/T_C for ferromagnetic materials with high elec-

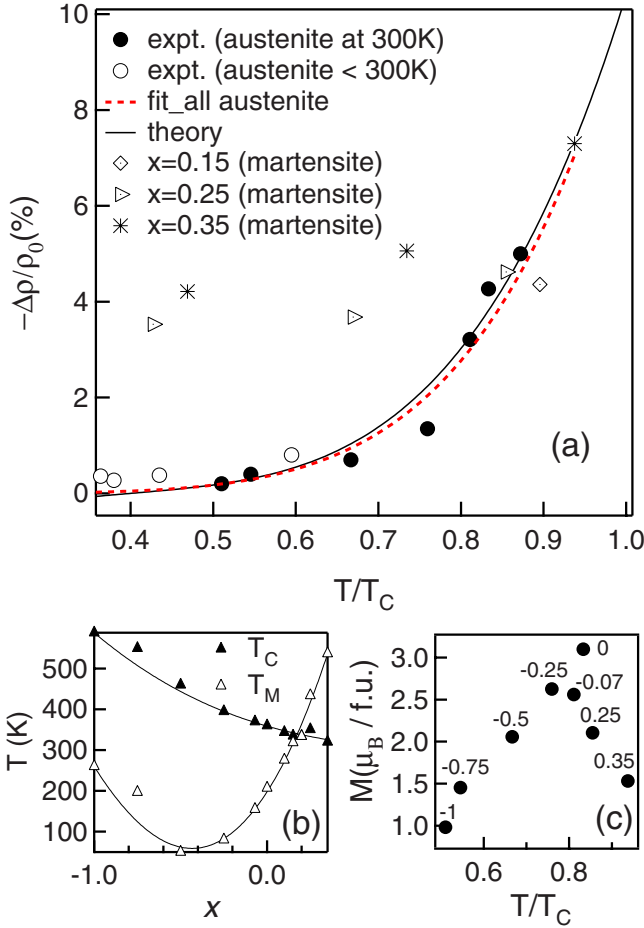


FIG. 2. (Color online) (a) The experimental MR data at 8 T for $\text{Ni}_{2+x}\text{Mn}_{1-x}\text{Ga}$ ($-1 \leq x \leq 0.35$) are plotted as a function of T/T_C , where $T \leq 300$ K and T_C varies with x as shown in (b). The experimental data are compared to the MR (solid line) derived from the theoretical calculation based on $s-d$ scattering model in Ref. 9. A least square fit to the experimental data for the austenitic phase (filled and open circles) is shown by red dashed line. (b) The martensitic start temperature (T_M) and Curie temperature (T_C) as a function of x . The solid lines serve as guide to the eyes. (c) Magnetization at 1 T at RT as a function of T/T_C . The x value for each data point is shown.

tron concentration. The $\text{Ni}_{2+x}\text{Mn}_{1-x}\text{Ga}$ compositions studied here have high electron concentration as given by the electron to atom ratio varying from 7.765 ($x=0.35$) to 6.75 ($x=-1$). These arguments indicate the applicability of the $s-d$ scattering model in Ref. 9 for $\text{Ni}_{2+x}\text{Mn}_{1-x}\text{Ga}$.

From Fig. 4 of Ref. 9, we have extracted the theoretical $\text{MR}(T/T_C)$ from the difference in $\rho(T/T_C)$ in zero and finite ($H/H_C=0.03$) external magnetic field. This is shown in Fig. 2(a) (solid line) and compared to experimental MR for the austenitic phase at $T \leq 300$ K. The agreement between the experiment and theory is good demonstrating that $s-d$ scattering is the dominant mechanism of MR in the austenitic phase. From Fig. 2(a), we clearly find that for $T/T_C \leq 0.5$, the $s-d$ scattering contribution to MR is negligible. Between 0.5 and 0.7 T_C , the increase in MR is small; but as T/T_C approaches 1, MR increases rapidly. In order to find an analytical expression that would describe MR variation with T/T_C , we have fitted the experimental data for the austenitic phase in Fig. 2(a) (filled circle for $T=300$ K and open circles for $T < 300$ K) with a model function: $c \times (T/T_C)^n$.

We allowed both c and n to vary freely in the least square error minimization algorithm, and obtain $c=10.4 \pm 1$ and $n=5.9 \pm 0.8 \approx 6$ [red dashed line in Fig. 2(a)]. The quality of the fit is good and the fitted curve is close to the theoretical curve (solid line) based on $s-d$ scattering model.⁹ Thus, it can be concluded that if MR is governed by $s-d$ scattering, in case of magnetic metals a $(T/T_C)^6$ variation of MR would be expected. Note that here T_C is composition dependent: decreases from 590 K ($x=-1$) to 320 K ($x=0.35$).

Now we turn to the discussion of MR in the martensitic phase *vis-a-vis* the $s-d$ scattering model. From Fig. 2(b), we find that $x=0.15$, 0.25, and 0.35 are in the martensitic phase at $T=300$ K with T/T_C values of 0.9, 0.85, and 0.94, respectively. Interestingly, the MR at 300 K for these compositions ($x=0.15-0.35$) fall close to the $s-d$ scattering curve within the experimental error [Fig. 2(a)]. This implies that close to T_C , the $s-d$ scattering dominates even in the martensitic phase. This is possibly because the martensitic transition in $\text{Ni}_{2+x}\text{Mn}_{1-x}\text{Ga}$ does not involve change in magnetic order and the change in total and local magnetic moments across the transition is rather small. For example, Ni_2MnGa is ferromagnetic in both the phases with total moments of $3.2\mu_B$ ($3.49\mu_B$) and Mn local moment of $2.74\mu_B$ ($2.83\mu_B$) in the austenitic (martensitic) phase.¹⁹ However, the magnetocrystalline anisotropy (MCA) exhibits a large increase at the martensitic transition,^{4,6,20} but unless the magnetic anisotropy energy density is larger than the product of maximal strain ($1-c/a$) and twinning stress, the magnetostructural effect (i.e., the electron scattering at twin boundaries and domain walls) on MR is not expected to be substantial.⁴ For $\text{Ni}_{2+x}\text{Mn}_{1-x}\text{Ga}$, as the temperature is lowered below T_M , the MCA in the martensitic phase increases²⁰ while as temperature decreases below T_C the $s-d$ scattering decreases [Fig. 2(a)]. So, at considerably lower temperatures compared with T_C and also T_M , MR deviates from the $s-d$ scattering model [Fig. 2(a)]. This is possibly related to the electron scattering at the twin and domain boundaries which appear in the martensitic phase. We show in Fig. 2(a) the deviation of MR measured at 235 K and below from the $s-d$ scattering model for $x=0.25$ ($T_M=434$ K, $T_C=351$ K) and $x=0.35$ ($T_M=537$ K, $T_C=320$ K). It may be noted however that for $x=0.15-0.35$, due to occurrence of the martensitic phase, the MR(H) deviates more from the linear behavior than in the other compositions ($x < 0.15$) studied here in the austenitic phase at RT [Fig. 1(a)]. The present finding that $s-d$ scattering is negligible for $T/T_C \leq 0.5$ explains our earlier result for $\text{Ni}_{1.75}\text{Mn}_{1.25}\text{Ga}$ ($x=-0.25$), where below 135 K ($T/T_C=0.35$) MR is governed by other mechanisms.⁴ Here, T_M is small ($=76$ K, i.e., $T_M/T_C=0.2$) and hence influence of $s-d$ scattering is negligible at T_M resulting in clear signature of magnetostructural effect at the martensitic transition.⁴ In fact, since it is a weak effect of magnitude less than 1% (Ref. 4), low temperature ($T \ll T_C$) is required. In Ref. 3, in the martensitic phase at 150 K ($T/T_C=0.4$) in the low field region, a cusplike shape and deviation from linearity was observed in MR for Ni_2MnGa ($T_M=207$ K, $T_C=365$ K), which was ascribed to electron scattering at the twin and domain boundaries.³

Although MR exhibits a monotonic variation with T/T_C

[Fig. 2(a)], the magnetization at RT [Fig. 1(b)] at 1 T does not. As shown in Fig. 2(c), it is highest for $x=0$ and it decreases for both Ni and Mn excess compositions. Experimentally, it is reported that the saturation magnetization is $3.8\mu_B$ for Ni_2MnGa ($x=0$),²¹ and decreases for both Ni excess (for $x=0.19$ it is around $3.4\mu_B$) and Mn excess (for $x=-1$ we find it to be $1.5\mu_B$) specimens.^{7,21} This behavior may have its origin in the differences in the magnetic ground state of the different $\text{Ni}_{2+x}\text{Mn}_{1-x}\text{Ga}$ compositions, as shown previously by *ab initio* spin polarized density functional theory calculations for Ni_2MnGa , Mn_2NiGa , and nonstoichiometric $\text{Ni}_{2.25}\text{Mn}_{0.75}\text{Ga}$.^{17,18,22,23} For $\text{Ni}_{2.25}\text{Mn}_{0.75}\text{Ga}$, the excess Ni atoms are ferromagnetically aligned with Mn, but their moments ($0.25\mu_B$) are smaller than Mn ($3.26\mu_B$).^{17,22} Thus, increase in Ni content at the expense of Mn that has higher magnetic moment decreases the total moment. In contrast, for Mn_2NiGa , there are two inequivalent Mn atoms whose moments are unequal and antiparallel resulting in a ferrimagnetic ground state with smaller moment.^{4,18} For ferrimagnetic metallic alloys such as $\text{Ni}_x(\text{Cu}+\text{Mn})_{1-x}$, the applicability of $s-d$ scattering has been discussed in literature,²⁴ and this justifies the good agreement obtained here between the MR of Mn excess Ni–Mn–Ga specimens with the theory based on $s-d$ scattering model in Ref. 9.

IV. CONCLUSIONS

To conclude, in this work we demonstrate that MR increases by more than one order of magnitude in $\text{Ni}_{2+x}\text{Mn}_{1-x}\text{Ga}$ at RT as the composition changes from $x=-1$ to 0.35. This finding might lead to the application of Ni–Mn–Ga as magnetic sensors where response to a particular magnetic field can be tuned through composition. The MR variation in the austenitic phase has been explained on the basis of theoretical calculations based on $s-d$ scattering model.⁹ A general expression for MR variation with T/T_C in magnetic metals where $s-d$ scattering mechanism is dominant is proposed.

ACKNOWLEDGMENTS

P. Chaddah, A. K. Raychaudhuri, A. Gupta, P. Nordblad, A. Banerjee, and K. Horn are thanked for constant support. Financial support from Max Planck Institute, Germany and Department of Science and Technology, Government of India are gratefully acknowledged.

- ¹K. Ullakko, J. K. Huang, C. Kantner, R. C. O’Handley, and V. V. Kokorin, *Appl. Phys. Lett.* **69**, 1966 (1996); S. J. Murray, M. Marioni, S. M. Allen, R. C. O’Handley, and T. A. Lograsso, *ibid.* **77**, 886 (2000).
- ²J. Marcos, L. Manosa, A. Planes, F. Casanova, X. Batlle, and A. Labarta, *Phys. Rev. B* **68**, 094401 (2003).
- ³C. Biswas, R. Rawat, and S. R. Barman, *Appl. Phys. Lett.* **86**, 202508 (2005).
- ⁴S. Banik, R. Rawat, P. K. Mukhopadhyay, B. L. Ahuja, A. Chakrabarti, P. L. Paulose, S. Singh, A. K. Singh, D. Pandey, and S. R. Barman, *Phys. Rev. B* **77**, 224417 (2008); S. Banik, R. Rawat, P. K. Mukhopadhyay, B. L. Ahuja, A. Chakrabarti, and S. R. Barman, *Adv. Mater. Res.* **52**, 207 (2008).
- ⁵X. Zhou, W. Li, H. P. Kunkel, and G. Williams, *J. Phys.: Condens. Matter* **16**, L39 (2004).
- ⁶S. Banik, A. Chakrabarti, U. Kumar, P. K. Mukhopadhyay, A. M. Awasthi, R. Ranjan, J. Schneider, B. L. Ahuja, and S. R. Barman, *Phys. Rev. B* **74**, 085110 (2006).
- ⁷G. D. Liu, J. L. Chen, Z. H. Liu, X. F. Dai, G. H. Wu, B. Zhang, and X. X. Zhang, *Appl. Phys. Lett.* **87**, 262504 (2005).
- ⁸I. Takeuchi, O. O. Famodu, J. C. Read, M. A. Aronova, K.-S. Chang, C. Craciunescu, S. E. Lofland, M. Wutting, F. C. Wellstood, L. Knauss, and A. Orozco, *Nature Mater.* **2**, 180 (2003).
- ⁹M. Kataoka, *Phys. Rev. B* **63**, 134435 (2001).
- ¹⁰S. Banik, R. Ranjan, A. Chakrabarti, S. Bhardwaj, N. P. Lalla, A. M. Awasthi, V. Sathe, D. M. Phase, P. K. Mukhopadhyay, D. Pandey, and S. R. Barman, *Phys. Rev. B* **75**, 104107 (2007).
- ¹¹R. Ranjan, S. Banik, S. R. Barman, U. Kumar, P. K. Mukhopadhyay, and D. Pandey, *Phys. Rev. B* **74**, 224443 (2006); B. L. Ahuja, G. Ahmed, S. Banik, M. Itou, Y. Sakurai, and S. R. Barman, *ibid.* **79**, 214403 (2009).
- ¹²V. O. Golub, A. Ya. Vovk, L. Malkinski, C. J. O’Connor, Z. Wang, and J. Tang, *J. Appl. Phys.* **96**, 3865 (2004).
- ¹³R. Mallik, E. V. Sampathkumaran, and P. L. Paulose, *Appl. Phys. Lett.* **71**, 2385 (1997).
- ¹⁴B. Raquet, M. Viret, E. Sondergard, O. Cespedes, and R. Mamy, *Phys. Rev. B* **66**, 024433 (2002).
- ¹⁵T. Kasuya, *Prog. Theor. Phys.* **16**, 58 (1956).
- ¹⁶J. Kübler, A. R. Williams, and C. B. Sommers, *Phys. Rev. B* **28**, 1745 (1983).
- ¹⁷S. R. Barman, S. Banik, and A. Chakrabarti, *Phys. Rev. B* **72**, 184410 (2005).
- ¹⁸S. R. Barman, S. Banik, A. K. Shukla, C. Kamal, and A. Chakrabarti, *Europhys. Lett.* **80**, 57002 (2007); S. R. Barman and A. Chakrabarti, *Phys. Rev. B* **77**, 176401 (2008).
- ¹⁹P. J. Brown, A. Y. Bargawi, J. Crangle, K.-U. Neumann, and K. R. A. Ziebeck, *J. Phys.: Condens. Matter* **11**, 4715 (1999).
- ²⁰F. Albertini, L. Pareti, A. Paoluzia, L. Morellon, P. A. Algarabel, M. R. Ibarra, and L. Righi, *Appl. Phys. Lett.* **81**, 4032 (2002).
- ²¹V. V. Khovailo, V. Novosad, T. Takagi, D. A. Filippov, R. Z. Levitin, and A. N. Vasil’ev, *Phys. Rev. B* **70**, 174413 (2004).
- ²²A. Chakrabarti, C. Biswas, S. Banik, R. S. Dhaka, A. K. Shukla, and S. R. Barman, *Phys. Rev. B* **72**, 073103 (2005).
- ²³B. L. Ahuja, B. K. Sharma, S. Mathur, N. L. Heda, M. Itou, A. Andrejczuk, Y. Sakurai, A. Chakrabarti, S. Banik, A. M. Awasthi, and S. R. Barman, *Phys. Rev. B* **75**, 134403 (2007).
- ²⁴I. Nicoară, *Phys. Status Solidi B* **77**, K17 (1976).